processes

Article

Performance Identification of a Steam Boiler Burner via Acoustic Analysis

Kayra Kurşun [1], Levent Özdemir [2] and Hakan Ersoy [1,*]

[1] Department of Mechanical Engineering, Akdeniz University, Antalya 07070, Turkey; kayrakursun@akdeniz.edu.tr
[2] Technical Directorate of Akdeniz University Hospital, Akdeniz University, Antalya 07070, Turkey; lozdemir@akdeniz.edu.tr
* Correspondence: hakanersoy@akdeniz.edu.tr

Abstract: Almost all systems generate acoustic signals when operating or when a process is being performed. These signals contain certain data related to the operating performance of systems. In this study, acoustic data were used to study the performance and to identify the optimum operating points of natural gas burners that are used in steam boilers. The sound recordings of burners obtained under different operating conditions were examined with acoustic analysis methods. The impact of various operating parameters on acoustic values was determined using time series analysis, frequency spectrum data and then power spectral density values. When the excess air coefficient and emission and efficiency values of boilers were compared with the acoustic data, it was determined that the Yule–Walker algorithm contained distinct and explanatory values. The steam boiler and the natural gas burner within were considered a system for the analysis. Measurement results showed that operating parameters and acoustic analysis results were correlated. Moreover, the results were confirmed with the emission measurement results. Finally, it was deduced that the acoustic values can be used for obtaining the optimum operating points in similar systems where inlet and outlet parameters cannot be measured, and the related principles were revealed.

Keywords: acoustics; steam boiler; steam trap; excess air coefficient; Fourier transformation; spectral analysis; autoregressive method; Yule–Walker

check for updates

Citation: Kurşun, K.; Özdemir, L.; Ersoy, H. Performance Identification of a Steam Boiler Burner via Acoustic Analysis. *Processes* **2022**, *10*, 1223. https://doi.org/10.3390/pr10061223

Academic Editors: Roberto Alonso González Lezcano, Francesco Nocera and Rosa Giuseppina Caponetto

Received: 5 May 2022
Accepted: 13 June 2022
Published: 20 June 2022

1. Introduction

The primary goal of employing time series in system analyses is to determine the state of the physical quantity being observed or investigated over time based on changing parameters, as well as to comprehend the nature of such data. The obtained data allow for predictions about the system's current state and potential future values. Furthermore, by examining and analyzing time series using various methods, it is possible to reach specific conclusions about the system parameters that constitute the time series. Preliminary values for detecting system failure, as well as vital data on the system's operating performance, can be obtained by examining the acoustic time series that occur during the operation. However, obtaining the essential conclusions from these raw data is a challenge. Therefore, significant results can only be obtained by employing specific methods on the measured signals and then conducting appropriate analyses.

In this study, the combustion performance data of the natural gas burner operating in conjunction with the steam boiler were studied by analyzing acoustic signals. Most studies in the literature considered the vibration data of the systems as time series and attempted to reach conclusions for performance and failure prevention in this manner. For instance, gearbox vibration data were used in studies related to detection of gear shaft and gear tooth failure. In these studies, autoregressive methods [1] and parametric methods [2] were used for modeling, and the Yule–Walker algorithm was used for parameter estimation [1,2].

Likewise, parametric methods also provided decent results in the formation and analysis of impact-induced vibration models [3]. Additionally, the Kolmogorov–Smirnov method is utilized to predict error signals [1,4]. On the other hand, in studies that focus more on steam boilers, combustion chambers or burners for failure detection, it is observed that the main problems of interest are related to leak detection, performance identification and combustion instability. In studies related to leak detection, model-based least squares technique [5] and principal component analysis are used [6]. For the matter of performance identification, acoustic data are used for analysis, and Yule–Walker algorithms are utilized for parameter estimation [7]. Apart from these, issues related to combustion instability are an area of interest in the literature. In this area, the static instability of the plasma arcs [8] and the combustion imbalances in the annulus burners of rotary kiln [9] are studied experimentally for swirl flame. In the case of thermo-acoustic instability [10,11], numerical and experimental methods [12–14], experimental flame transfer functions [15,16], large eddy simulations [17,18], fast random particle method [19] and nonlinear network models [20,21] are used. To provide the passive control of thermo-acoustic instability, the slope confinement method is utilized [22]. In addition, the acoustic emission method, which, in recent years, needs less data [23], is used for failure detection in the tubes of steam generators, boilers and heat exchangers [24]. Moreover, bidirectional long short-term memory recurrent neural networks [25] and the deep learning flexible boundary regression method can be used with acoustic emission signals to enhance leak detection in boiler tubes [26]. Acoustic array global interpolation algorithms have been developed for leak detection during boiler operations of coal-fired power plants [27].

In this study, it has been shown that acoustic methods can be used to obtain optimum operating performance in terms of gas emissions and fuel efficiency. Spectral analysis methods were applied to produce optimum air excess coefficient settings of steam boilers and burners. It was observed that combustion adjustments can be made through acoustic analysis, especially in cases where classical measurement methods cannot be performed.

2. Materials and Methods

The spectral analysis method explains the power distribution of a signal (such as sound and vibration) in a finite data set. This method can be used in various applications such as the detection of embedded signals in a wide band interval. Spectrum analysis in signal processing can be basically classified as parametric and non-parametric methods. In non-parametric methods, power spectrum density (PSD) is directly obtained from the signal itself, and the simplest of these is the periodogram. The developed form of periodogram is based on Welch's method and the multitaper method. In parametric methods, the PSD is obtained from a linear system. The most commonly known algorithms of this method are the Yule–Walker autoregressive method and the Burg method. These methods try to obtain the parameters (coefficients) of the linear system to determine the PSD. Then, they generate a signal based on the assumption. These methods yield better results than conventional non-parametric methods if the signal duration is short. Moreover, parametric methods can achieve higher resolution values compared to non-parametric methods [28]. Because the data of a system are depicted as X_n, the spectral power density of a random fixed process is related to the correlation series of a discrete Fourier transformation. This expression, in terms of normalized frequency, is as follows.

$$X(\omega) = \frac{1}{2\pi} \sum_{n=-\infty}^{\infty} x(n) e^{-jn\omega} \tag{1}$$

where the normalized frequency is $\omega = 2\pi f/f_s$, f is the physical frequency, and f_s is the sampling frequency.

$$X(f) = \frac{1}{f_s} \sum_{n=-\infty}^{\infty} \frac{x(n) e^{-2\pi j f n}}{f_s} \tag{2}$$

Correlation series can be obtained from the spectral power density using the inverse of the discrete time Fourier transformation.

$$X(n) = \int_{-n}^{n} \left(x(\omega)e^{j\omega n} \right) d\omega = \int_{-\frac{f_s}{2}}^{\frac{f_s}{2}} \left(x(f)e^{\frac{2\pi j f n}{s}} \right) df \tag{3}$$

The average power of the $X(n)$ series within a certain data range is expressed by the following equation.

$$X(0) = \int_{-\pi}^{\pi} x(\omega)d\omega = \int_{\frac{f_s}{2}}^{\frac{f_s}{2}} x(f)df \tag{4}$$

The average power of a signal on a certain frequency band, $[\omega_1, \omega_2]$, $0 \leq \omega_1 < \omega_2 \leq \pi$, can be determined by taking the integral of the spectral power density over this band.

$$x_{[\omega_1,\omega_2]} = \int_{\omega_1}^{\omega_2} x(\omega)d\omega + \int_{-\omega_2}^{-\omega_1} x(\omega)d\omega \tag{5}$$

In Equation (5), this expression, which represents the power content of a signal in $x(\omega)$ infinitely low frequency band, is called the spectral power density. In reality, PSDs of signals are symmetrical. Therefore, $x(\omega)$ entirely represents the PSD in the interval $0 \leq \omega < \pi$. Of the spectral estimation methods, the Yule–Walker AR method calculates the AR parameters of a signal generated with the partial prediction of its "autoregressive" function and calculates the forward prediction error with the minimization of the smallest squares. Equation (6) is known as the Yule–Walker equation and forms the basis of many AR prediction methods [29].

$$\begin{bmatrix} r(1) & r(2) & \cdots & r(p) \\ r(2) & r(1) & \cdots & r(p-1) \\ \vdots & \vdots & \cdots & \vdots \\ r(p) & \cdots & r(2) & r(1) \end{bmatrix} \begin{Bmatrix} a(2) \\ a(3) \\ \vdots \\ a(p+1) \end{Bmatrix} = \begin{Bmatrix} -r(2) \\ -r(3) \\ \vdots \\ -r(p+1) \end{Bmatrix} \tag{6}$$

The Yule–Walker AR method generates results like a maximum entropy estimator. Using a method against the autocorrelation function ensures that the autocorrelation matrix in Equation (6) is positive. Therefore, the matrix can be reversed, and it can guarantee an existing solution. Moreover, these calculated AR parameters always result in a stable all-pole model. The Yule–Walker equations make use of the Toeplitz structure, which is an autocorrelation matrix and is efficiently solved using the Levinson algorithm. This is a matrix, and each member, from left to right diagonally, is fixed.

Experimental Setup

Measurements were taken on an industrial-type steam boiler installed in the university hospital. The steam boiler technical specifications were as follows: capacity max. 6800 kW; operating pressure 7 Bar; water volume 25,000 L; burner capacity max. 8000 kW; fuel type, natural gas; motor power, 30 kW. Moreover, the steam boiler uses natural gas as fuel and has an Oertili induflame burner. A Testo 330-2LL (Testo, Istanbul, Turkey) device was used to measure the flue gas emissions. The calibration of this device was set to maximum. A composition of 3% O_2 and 12% CO_2 was used, and a AKG perception 170 cardioid condenser microphone was used for the acoustic data. Data were transferred to the computer via a Behringer-1222 FX preamp (Behringer, Willich, Germany) with 48 V phantom power supply. The Goldwave program (v5.10, St. John's, NL, Canada) was used in the preprocessing of the data; all other analyses and calculations were made using Matlab (v9.8 Academic, Mathworks, Natick, MA, USA, Source: Akdeniz University, IT Department, Antalya, Turkey). Before beginning the measurements, the boiler was operated for ~40 min, and the system was made to reach a stable state. For the comparability of the measurements, adjustments were made during all measurements, such that the steam boiler pressure was 6 bars and the frequency value of the primary air fan with frequency inverter was 25.7 Hz (Figure 1).

Figure 1. Boiler under measurement and test set-up.

3. Results

Measurements of the system were made for eight different excess air coefficients at 16 bits. The presence of three sound sources was assumed in the system during the acoustic recordings: the data coming from the primary air fan, the sound of natural gas flow and the acoustic data during burning in the combustion chamber. The acoustic data in the combustion chamber were subjected to acoustic analyses after they was separated from the noise coming from the other two sources. It was observed that the system worked stably during the steady regime; therefore, it was concluded that a measurement interval of 10 s was sufficient. When the acoustic recordings were being made, flue gas emissions and efficiency values of the system were simultaneously determined. Figure 2 shows the time–amplitude values of the acoustic data obtained from the recordings for the eight different excess air coefficients. Here, fluctuations depending on the combustion state are reflected in the graphics. Subsequently, these values were transferred from time domain to frequency domain for each excess air coefficient. Figure 3 shows the expansions of signals on the frequency axis.

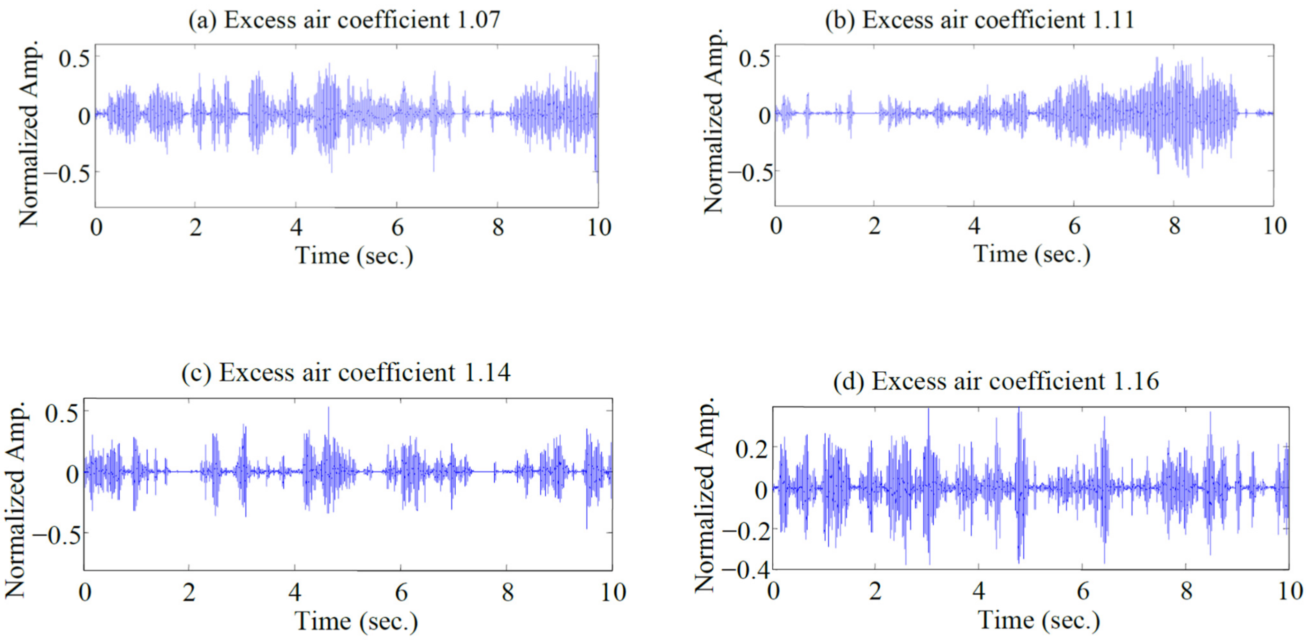

Figure 2. *Cont.*

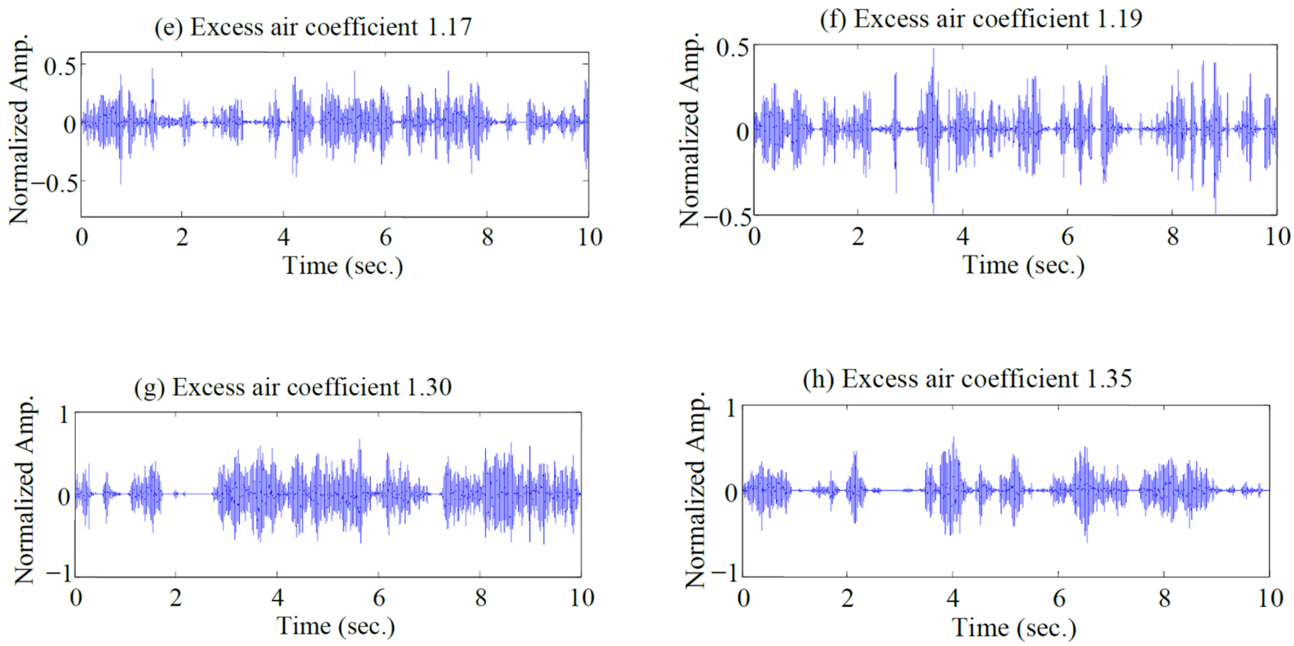

Figure 2. Measurement data obtained for the excess air coefficients.

While recording acoustic data, changes were made in the λ excess air coefficient values and flue gas emissions, and boiler efficiency values were simultaneously measured for each excess air coefficient value. These values are listed in Table 1. When the emission and efficiency values were examined, the measurement number 3 corresponding to λ = 1.14 value was more balanced compared to other parameters; it was decided that it could be considered a reference. The excess air coefficient of 1.14 of the boiler measured at the third measurement was determined as the excess air coefficient where combustion is the most suitable, as per the criteria set by standards regarding flue gas emissions and efficiency values. When determining this value, an evaluation was made among emission values and efficiency values in Table 1, and the balance between emission and efficiency values was considered. This designated value was considered as a reference for other measurements.

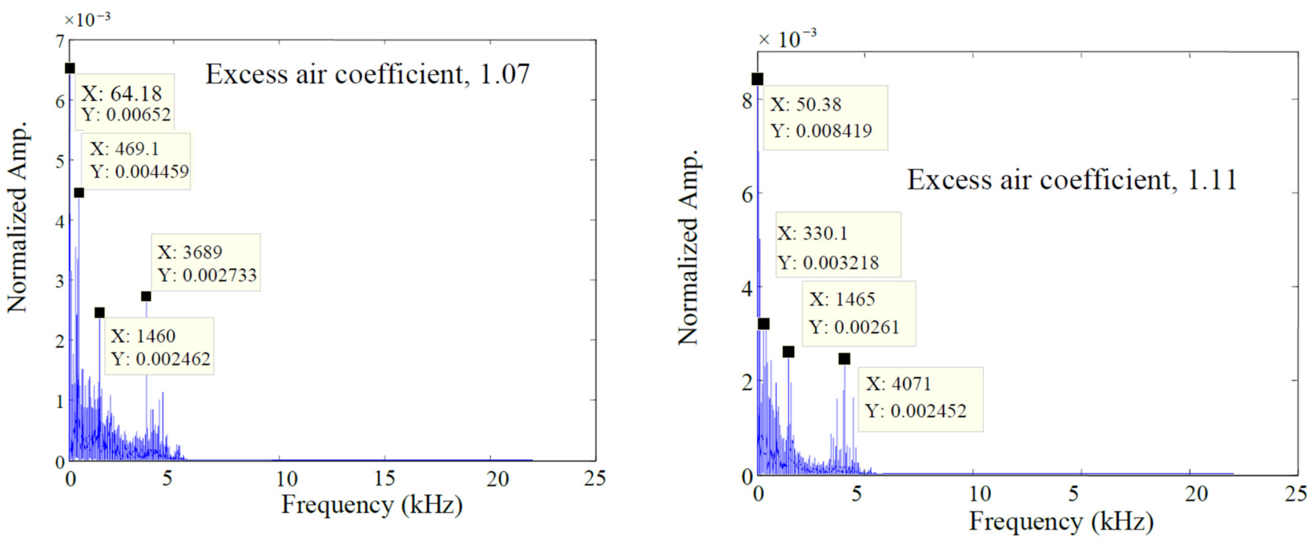

Figure 3. *Cont.*

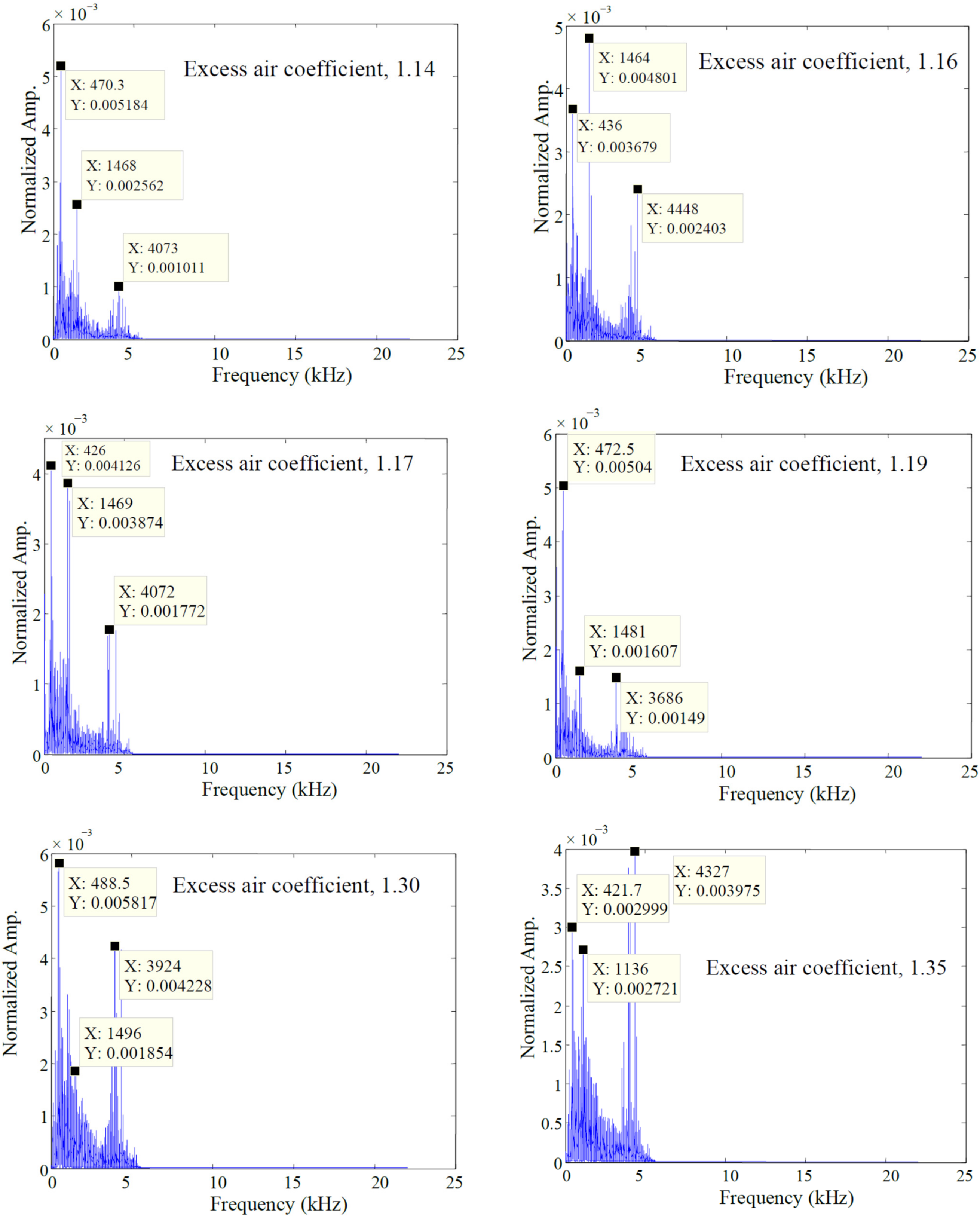

Figure 3. Frequency distributions of measurements taken for the excess air coefficients.

Table 1. Flue gas emission values and boiler efficiency for the excess air coefficient λ values.

Measurement	1	2	3	4	5	6	7	8
λ	1.07	1.11	1.14	1.16	1.17	1.19	1.30	1.35
O_2%	1.3	2.0	2.5	2.9	3.1	3.3	4.8	5.5
CO_2%	11.26	10.86	10.57	10.34	10.23	10.11	9.26	8.86
CO%	199	81	14	7	4	5	0	0
Efficiency %	93.8	93.8	93.6	93.5	93.4	93.5	93.0	92.6

Yule–Walker power spectral density values with respect to the excess air values are given in Table 2.

Table 2. Yule–Walker power spectral density values corresponding to excess air values.

Measurement	1	2	3	4	5	6	7	8
λ	1.07	1.11	1.14	1.16	1.17	1.19	1.30	1.35
x1	775.1	602.9	689.1	1034.0	947.5	516.8	947.5	1120.0
x2	3962	3962	3704	3962	3962	3962	4048	4048
y1/y2	13.02	22.29	22.77	14.87	2.25	2.84	8.55	4.28

If we consider the acoustic data as a time series, the recordings were made for eight different excess air coefficients in time slices of 10 s (Figure 2). From this data, the distribution in frequency domain was obtained through the fast Fourier transform process (Figure 3). Using the obtained frequency data, the distribution of PSD values in frequency domain was found using the Yule–Walker algorithm (Figure 4). In the PSD graphs, the peak frequencies for normalized values were examined. By making power density calculations, it was determined at which frequencies the data were concentrated (Figure 5).

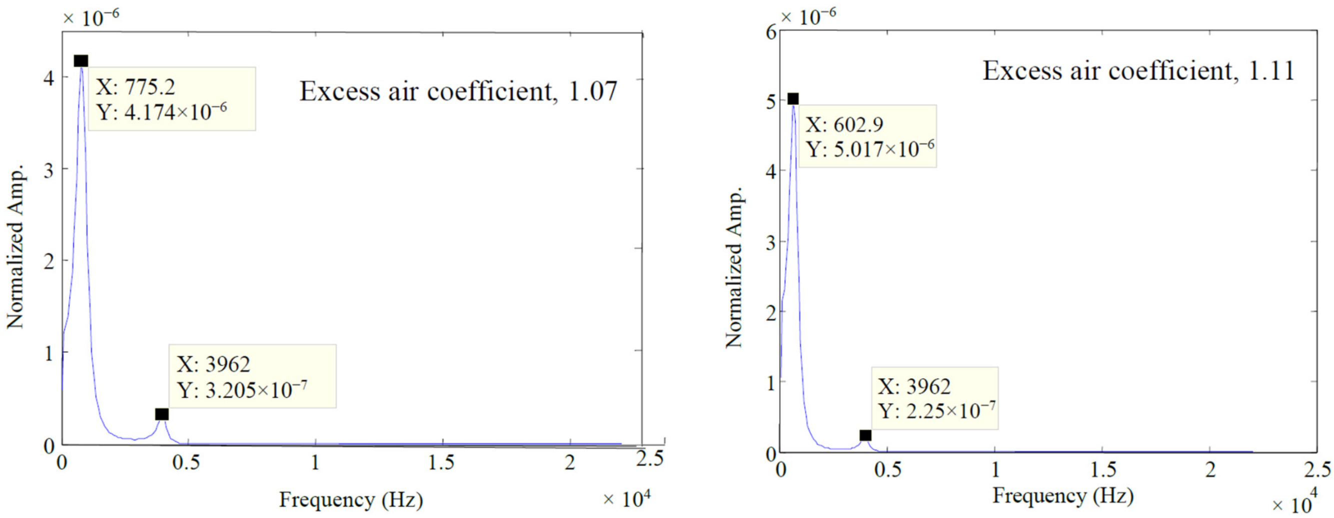

Figure 4. *Cont.*

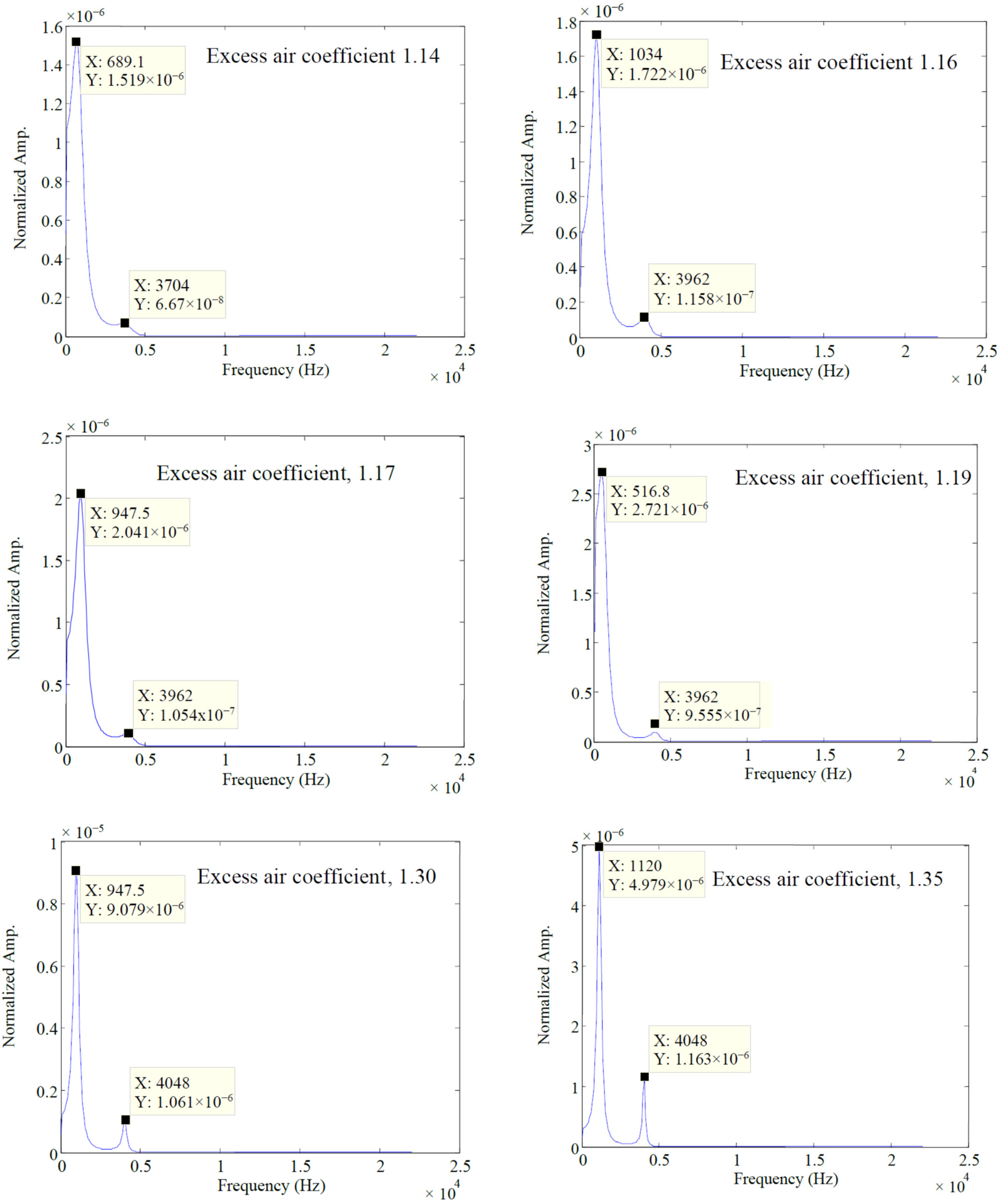

Figure 4. Yule–Walker power spectral density values.

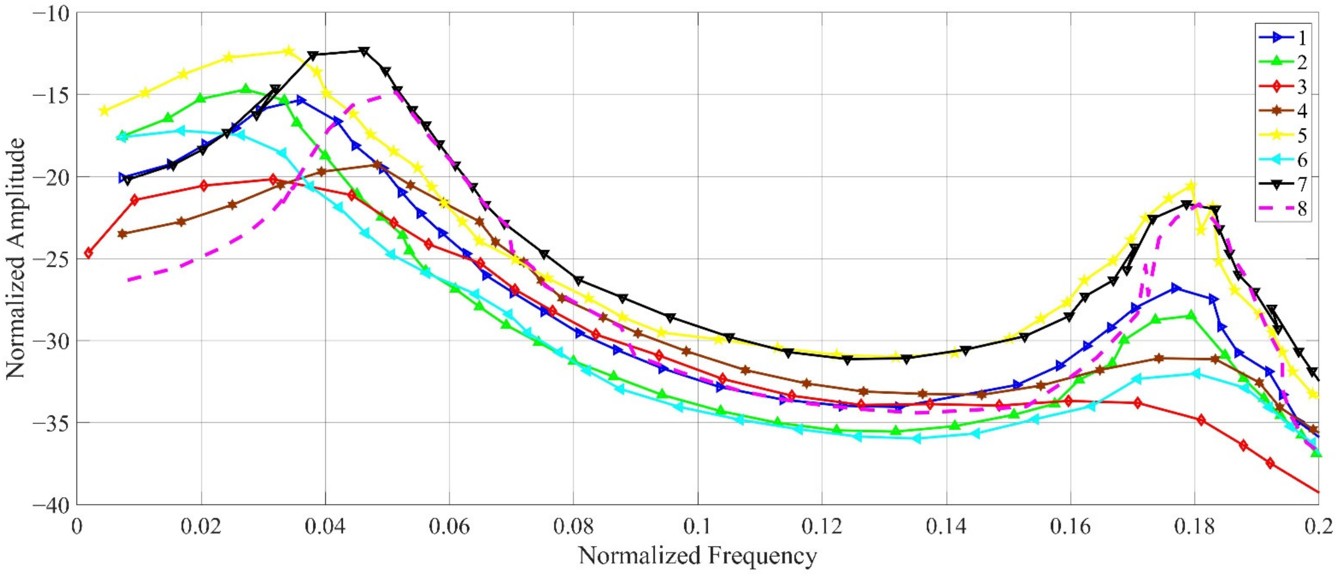

Figure 5. Yule-Walker Power Spectral Density.

4. Discussion

Time graphs of acoustic data were plotted for eight different excess air coefficients, and then their frequency spectra were obtained. PSD values were calculated and plotted for these values. Furthermore, other parametric methods, namely Burg, covariance and modified covariance methods, were also examined. In the data obtained within the scope of the study, it was determined that the "Yule–Walker" method has some advantages over other methods; it is also possible to apply windowing to acoustic signals, and these data can be recorded as larger datasets compared to other methods. When the Figure 5 plot comprising the power spectra of the acoustic signals obtained for each of the eight residual air coefficients was examined, the curve around the first and second peak values showed that the combustion was in the best condition. In other areas of the spectrum, a decrease and a stable situation were observed. Therefore, it was concluded that the Yule–Walker method is more suitable for these data characteristics and analyses, and plots were made using the Yule–Walker method. Table 2 shows the frequencies at which the peak points of PSD values occur for each excess air coefficient and yields the PSD ratios of the two peak points as y1/y2. In the literature, thermoacoustic instability of a large-scale industrial oil furnace was studied using acoustic data, turbulence energy spectrum and Rayleigh parameter, across the domain in [17]. At the maximum continuous rating load, all three methods predict instability with fluctuations of the predicted dominant frequencies in agreement with the observed nondimensional frequency of 0.615. Here, the measurement made for the excess air coefficient of 1.14 stands out from the others with its higher value. Moreover, this value corresponds to the value of 1.14, which may be considered the optimum value compared with the emission and efficiency values in Table 1. When the values obtained with the Yule–Walker algorithm are examined in Figure 5, the curve number 3 belonging to the excess air coefficient of 1.14 stands out because of its lower relative peak points.

5. Conclusions

In this study, the operating parameters of the natural gas boiler's burner were evaluated along with acoustic data. Law emission values for internal combustion engines are not at points where the engine power and efficiency are at their optimum values, and an optimum operating point must be determined among these values. A similar situation is observed for gas burners. This study has shown that this optimum point can be determined using acoustic data. Acoustic data can be easily used in systems where it is impossible or very difficult to measure operating parameters. Furthermore, analyses can be made in many systems with acoustic data that can be measured much more easily. Furthermore, in many cases, acoustic data contain considerably more information about the system. In this study, the Yule–Walker PSD values can be applied to the steam boiler with natural gas burner and correlated with the performance values of the boiler such as emission and efficiency; moreover, such analyses can be used for improving the boiler performance. In particular, parametric methods will be an important analysis method for optimizing combustion parameters.

Author Contributions: Conceptualization, K.K. and H.E.; methodology, L.Ö. and H.E.; experimental setup, L.Ö. and K.K.; validation, K.K. and H.E.; formal analysis, K.K.; investigation, K.K. and L.Ö.; resources, K.K. and H.E.; data curation, H.E.; writing—original draft preparation, L.Ö. and K.K.; writing—review and editing, K.K. and L.Ö.; visualization, K.K. and L.Ö.; supervision, H.E.; project administration, L.Ö. and H.E.; funding acquisition, H.E. All authors have read and agreed to the published version of the manuscript.

Funding: This work was supported by The Scientific Research Projects Coordination Unit of Akdeniz University. Project Number: FDK-2021-5619.

Institutional Review Board Statement: Not applicable.

Informed Consent Statement: Not applicable.

Data Availability Statement: The data presented in this study are available on request from the corresponding author.

Conflicts of Interest: The authors declare no conflict of interest.

Nomenclature

$x(n)$	Time series
$X(f)$	Fourier transform
f_s	Sampling frequency
f	Frequency
ω	Angular frequency
$r(p)$	Autocorrelation function

References

1. Wang, X.; Makis, V. Autoregressive model-based gear shaft fault diagnosis using the Kolmogorov–Smirnov test. *J. Sound Vib.* **2009**, *327*, 413–423. [CrossRef]
2. Ettefagh, M.M.; Sadeghi, M.H.; Rezaee, M.; Chitsaz, S. Latent component-based gear tooth fault detection filter using advanced parametric modeling. *Mech. Syst. Signal Process.* **2009**, *23*, 2260–2286. [CrossRef]
3. Ettefagh, M.M.; Sadeghi, M.H.; Rezaee, M.; Khoshbakhti, R.; Akbarpour, R. Application of a new parametric model-based filter to knock intensity measurement. *Measurement* **2010**, *43*, 353–362. [CrossRef]
4. Kar, C.; Mohanty, A.R. Multistage gearbox condition monitoring using motor current signature analysis and Kolmogorov–Smirnov test. *J. Sound Vib.* **2006**, *290*, 337–368. [CrossRef]
5. Sun, X.; Chen, T.; Marquez, H.J. Efficient model-based leak detection in boiler steam-water systems. *Comput. Chem. Eng.* **2002**, *26*, 1643–1647. [CrossRef]
6. Sun, X.; Marquez, H.J.; Chen, T.; Riaz, M. An improved PCA method with application to boiler leak detection. *ISA Trans.* **2005**, *44*, 379–397. [CrossRef]
7. Özdemir, L. Performance Identification of Steam Heating Systems by Acoustic Analyses. Master's Thesis, Akdeniz University, Antalya, Turkey, 2013.
8. Chen, W.; Jin, D.; Cui, W.; Huang, S. Characteristics of gliding arc plasma and its application in swirl flame static instability control. *Processes* **2020**, *8*, 684. [CrossRef]
9. Elattar, H.F.; Specht, E.; Fouda, A.; Rubaiee, S.; Al-Zahrani, A.; Nada, S.A. Swirled Jet Flame Simulation and Flow Visualization Inside Rotary Kiln—CFD with PDF Approach. *Processes* **2020**, *8*, 159. [CrossRef]
10. Gangisetty, G.; Jayachandran, A.T.; Sverbilov, V.Y.; Zubrilin, I.; Matveev, S. Review paper on thermo-acoustic instabilities in a gas turbine burners–Flashback avoidance. *J. Phys. Conf. Ser.* **2019**, *1276*, 012051. [CrossRef]
11. Beita, J.; Talibi, M.; Sadasivuni, S.; Balachandran, R. Thermoacoustic Instability Considerations for High Hydrogen Combustion in Lean Premixed Gas Turbine Combustors: A Review. *Hydrogen* **2021**, *2*, 33–57. [CrossRef]
12. Hou, S.-S.; Chung, D.-H.; Lin, T.-H. Experimental and numerical investigation of jet flow and flames with acoustic modulation. *Int. J. Heat Mass Transf.* **2015**, *83*, 562–574. [CrossRef]

13. Kraus, C.; Harth, S.; Bockhorn, H. Experimental investigation of combustion instabilities in lean swirl-stabilized partially-premixed flames in single- and multiple-burner setup. *Int. J. Spray Combust. Dyn.* **2016**, *8*, 4–26. [CrossRef]
14. Laera, D.; Camporeale, S.M. A Weakly Nonlinear Approach Based on a Distributed Flame Describing Function to Study the Combustion Dynamics of a Full-Scale Lean-Premixed Swirled Burner. *J. Eng. Gas Turbines Power* **2017**, *139*, 091501. [CrossRef]
15. Berger, F.M.; Hummel, T.; Hertweck, M.; Kaufmann, J.; Schuermans, B.; Sattelmayer, T. High-Frequency Thermoacoustic Modulation Mechanisms in Swirl-Stabilized Gas Turbine Combustors—Part I: Experimental Investigation of Local Flame Response. *J. Eng. Gas Turbines Power* **2017**, *139*, 071501. [CrossRef]
16. Weng, F.; Li, S.; Zhong, D.; Zhu, M. Investigation of self-sustained beating oscillations in a Rijke burner. *Combust. Flame* **2016**, *166*, 181–191. [CrossRef]
17. Kim, D.; Park, Y.; You, D.; Huh, K.Y. Analysis of thermoacoustic instability with corresponding eigenfrequencies in a large scale industrial oil furnace. *J. Mech. Sci. Technol.* **2016**, *30*, 4979–4988. [CrossRef]
18. Kraus, C.; Selle, L.; Poinsot, T.; Arndt, C.M.; Bockhorn, H. Influence of Heat Transfer and Material Temperature on Combustion Instabilities in a Swirl Burner. *J. Eng. Gas Turbines Power* **2017**, *139*, 051503. [CrossRef]
19. Grimm, F.; Ohno, D.; Noll, B.; Aigner, M.; Ewert, R.; Dierke, J. Broadband Combustion Noise Simulation of the PRECCINSTA Burner Based on Stochastic Sound Sources. *J. Eng. Gas Turbines Power* **2017**, *139*, 011505. [CrossRef]
20. Bothien, M.R.; Noiray, N.; Schuermans, B. Analysis of Azimuthal Thermo-acoustic Modes in Annular Gas Turbine Combustion Chambers. *J. Eng. Gas Turbines Power* **2015**, *137*, 061505. [CrossRef]
21. Yang, F.; Guo, Z.; Fu, X.; Yu, D. Computation of acoustic transfer matrices of swirl burner with finite element and acoustic network method. *J. Low Freq. Noise Vib. Act. Control* **2015**, *34*, 169–184. [CrossRef]
22. Song, H.; Lin, Y.; Han, X.; Yang, D.; Zhang, C.; Sung, C.-J. The thermoacoustic instability in a stratified swirl burner and its passive control by using a slope confinement. *Energy* **2020**, *195*, 116956. [CrossRef]
23. Vicuña, C.M.; Höweler, C. A method for reduction of Acoustic Emission (AE) data with application in machine failure detection and diagnosis. *Mech. Syst. Signal Process.* **2017**, *97*, 44–58. [CrossRef]
24. Baofu, L.; Upadhyaya, B.R.; Perez, R.B. Structural integrity monitoring of steam generator tubing using transient acoustic signal analysis. *IEEE Trans. Nucl. Sci.* **2005**, *52*, 484–493. [CrossRef]
25. Ramezani, M.G.; Hasanian, M.; Golchinfar, B.; Saboonchi, H.; Zonta, D.; Huang, H. Automatic boiler tube leak detection with deep bidirectional LSTM neural networks of acoustic emission signals. In Proceedings of the Sensors and Smart Structures Technologies for Civil, Mechanical, and Aerospace Systems, Online Only, 27 April–9 May 2020.
26. Duong, B.P.; Kim, J.; Kim, C.-H.; Kim, J.-M. Deep Learning Object-Impulse Detection for Enhancing Leakage Detection of a Boiler Tube Using Acoustic Emission Signal. *Appl. Sci.* **2019**, *9*, 4368. [CrossRef]
27. Zhang, S.; Shen, G.; An, L. Leakage location on water-cooling wall in power plant boiler based on acoustic array and a spherical interpolation algorithm. *Appl. Therm. Eng.* **2019**, *152*, 551–558. [CrossRef]
28. Şeker, M.; Tokmakçi, M.; Asyali, M.H.; Seğmen, H. Examining EEG signals with parametric and non-parametric analyses methods in migraine patients during pregnancy. In Proceedings of the 2010 15th National Biomedical Engineering Meeting, Antalya, Turkey, 21–24 April 2010; IEEE: Piscataway Township, NJ, USA, 2010; pp. 1–4.
29. Stoica, P.; Moses, R.L. *Spectral Analysis of Signals*; Prentice Hall: Hoboken, NJ, USA, 2005.